

## Clickable NAD Analogues for Labeling Substrate Proteins of Poly(ADP-ribose) Polymerases

Hong Jiang,<sup>†</sup> Jun Hyun Kim,<sup>†</sup> Kristine M. Frizzell,<sup>‡</sup> W. Lee Kraus,<sup>‡,§</sup> and Hening Lin<sup>\*†</sup>

Department of Chemistry and Chemical Biology, Cornell University, Ithaca, New York 14850,  
Department of Molecular Biology and Genetics, Cornell University, Ithaca, New York 14850,  
and Department of Pharmacology, Weill Medical College of Cornell University,  
New York, New York 10021

Received March 4, 2010; E-mail: hl379@cornell.edu

**Abstract:** Poly(ADP-ribose) polymerases (PARPs) catalyze the transfer of multiple adenine diphosphate ribose (ADP-ribose) units from nicotinamide adenine dinucleotide (NAD) to substrate proteins. There are 17 PARPs in humans. Several PARPs, such as PARP-1 and Tankyrase-1, are known to play important roles in DNA repair, transcription, mitosis, and telomere length maintenance. To better understand the functions of PARPs at a molecular level, it is necessary to know what substrate proteins PARPs modify. Here we report clickable NAD analogues that can be used to label PARP substrate proteins. The clickable NAD analogues have a terminal alkyne group which allows the conjugation of fluorescent or affinity tags to the substrate proteins. Using this method, PARP-1 and tankyrase-1 substrate proteins were labeled by a fluorescent tag and visualized on SDS-PAGE gel. Using a biotin affinity tag, we were able to isolate and identify a total of 79 proteins as potential PARP-1 substrates. These include known PARP-1 substrate proteins, including histones and heterogeneous nuclear ribonucleoproteins. About 40% of the proteins were also identified in recent proteomic studies as potential PARP-1 substrates. Among the identified potential substrates, we further demonstrated that tubulin and three mitochondrial proteins, TRAP1 (TNF receptor-associated protein 1), citrate synthase, and GDH (glutamate dehydrogenase 1), are substrates of PARP-1 *in vitro*. These results demonstrate that the clickable NAD analogue is useful for labeling, in-gel detection, isolation, and identification of the substrate proteins of PARPs and will help to understand the biological functions of PARPs.

### Introduction

Poly(ADP-ribosylation) is the addition of multiple ADP-ribosyl groups from NAD to substrate proteins.<sup>1–3</sup> The first ADP-ribosyl group is added to the carboxylate side chain of Glu or Asp residues of the substrate proteins, followed by addition of more ADP-ribosyl groups to the 2'-OH groups of the two ribose rings (Figure 1), leading to long and branched poly(ADP-ribose) chains (PAR) that can contain hundreds of ADP-ribose units. The large size and the enormous negative charges of PAR chains can affect protein structure and function and thus regulate the biological processes in which the substrate proteins are involved. The enzymes that catalyze poly(ADP-ribosylation) are termed poly(ADP-ribose) polymerases, or PARPs. Seventeen PARPs have been identified in humans.<sup>1,4</sup> Of the 17 PARPs identified, only two of them, PARP-1 and Tankyrase-1, are relatively well studied. PARP-1 is found to

be required for DNA repair/genome maintenance<sup>5–7</sup> and transcriptional regulation of certain genes<sup>8–11</sup> by poly(ADP-ribosylation) of itself and many nucleosomal or nucleosome-associated proteins. It is also responsible for the induction of cell death under extreme stress (such as excessive DNA damage)<sup>12,13</sup> or pathological conditions (stroke, ischemia, diabetes).<sup>14–16</sup> Tankyrase-1 is known to be required for mitosis and telomere length maintenance by modifying the nuclear mitotic apparatus protein (NuMA)<sup>17–20</sup> and a telomere-binding

<sup>†</sup> Department of Chemistry and Chemical Biology, Cornell University.

<sup>‡</sup> Department of Molecular Biology and Genetics, Cornell University.

<sup>§</sup> Weill Medical College of Cornell University.

- (1) Schreiber, V.; Dantzer, F.; Ame, J.-C.; de Murcia, G. *Nat. Rev. Mol. Cell Biol.* **2006**, *7*, 517–528.
- (2) D'Amours, D.; Desnoyers, S.; D'Silva, I.; Poirier, G. G. *Biochem. J.* **1999**, *342*, 249–268.
- (3) Lin, H. *Org. Biomol. Chem.* **2007**, *5*, 2541–2554.
- (4) Amé, J.-C.; Spenlehauer, C.; Murcia, G. d. *BioEssays* **2004**, *26*, 882–893.

- (5) Poirier, G. G.; Murcia, G. D.; Jongstra-Bilen, J.; Niedergang, C.; Mandel, P. *Proc. Natl. Acad. Sci. U.S.A.* **1982**, *79*, 3423–3427.
- (6) de Murcia, G.; Huletsky, A.; Lamarre, D.; Gaudreau, A.; Pouyet, J.; Daune, M.; et al. *J. Biol. Chem.* **1986**, *261*, 7011–7017.
- (7) Althaus, F. R. *J. Cell Sci.* **1992**, *102*, 663–670.
- (8) Kim, M. Y.; Mauro, S.; Gevry, N.; Lis, J. T.; Kraus, W. L. *Cell* **2004**, *119*, 803–814.
- (9) Tulin, A.; Spradling, A. *Science* **2003**, *299*, 560–562.
- (10) Ju, B.-G.; Lunyak, V. V.; Perissi, V.; Garcia-Bassets, I.; Rose, D. W.; Glass, C. K.; et al. *Science* **2006**, *312*, 1798–1802.
- (11) Kraus, W. L. *Curr. Opin. Cell Biol.* **2008**, *20*, 294–302.
- (12) Yu, S.-W.; Wang, H.; Poitras, M. F.; Coombs, C.; Bowers, W. J.; Federoff, H. J.; et al. *Science* **2002**, *297*, 259–263.
- (13) Yu, S.-W.; Andrabi, S. A.; Wang, H.; Kim, N. S.; Poirier, G. G.; Dawson, T. M.; et al. *Proc. Natl. Acad. Sci. U.S.A.* **2006**, *103*, 18314–18319.
- (14) Burkle, A. *BioEssays* **2001**, *23*, 795–806.
- (15) Haince, J.-F.; Rouleau, M.; Hendzel, M. J.; Masson, J.-Y.; Poirier, G. G. *Trends Mol. Med.* **2005**, *11*, 456–463.
- (16) Virag, L.; Szabo, C. *Pharmacol. Rev.* **2002**, *54*, 375–429.

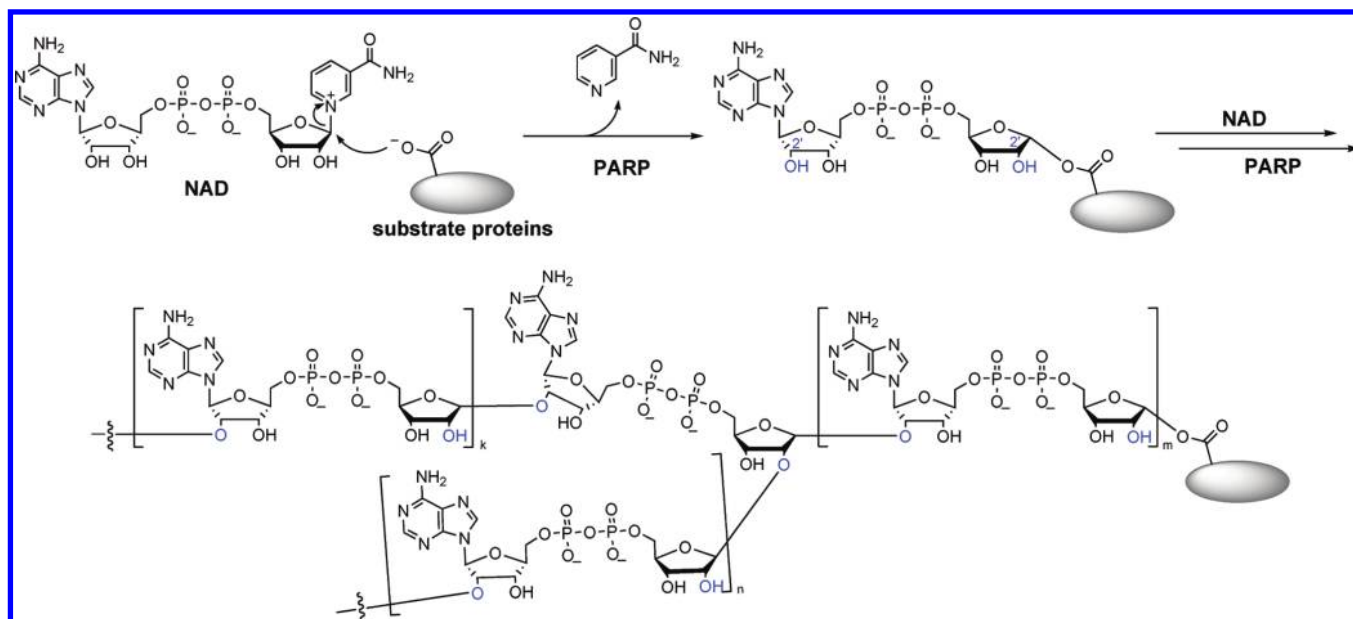


**Figure 1.** Poly(ADP-ribosylation) reaction catalyzed by PARPs.

protein TRF1.<sup>21,22</sup> The important biological functions of PARP-1 and Tankyrase-1 suggest that other PARPs could be likewise important. However, very little is known about other PARPs.

To understand the biological function of different PARPs, it is necessary to find out what substrate proteins are modified by different PARPs, similar to the efforts that have been invested in identifying kinase substrates.<sup>23,24</sup> At present, <sup>32</sup>P-NAD and PAR antibodies are the major methods used to detect protein poly(ADP-ribosylation). For isolation and identification of substrate proteins of PARPs, using PAR antibodies is the preferred option because the use of <sup>32</sup>P-NAD does not provide an affinity tag for isolation and purification. Recently, macro domain that can bind to ADP-ribose was used to isolate ADP-ribosylated proteins.<sup>25</sup> A major concern about using PAR antibodies and macro domains to identify substrate proteins is that the immunoprecipitation step is executed under native conditions and thus some nonsubstrate proteins that interact with a poly(ADP-ribosylated) protein will also be pulled down. This will give false positive results. Thus, new and improved methods to label and identify PARP substrate proteins are still needed.

Here, we report the use of clickable alkyne-tagged NAD analogues for labeling and identifying PARP substrate proteins (Figure 2). The terminal alkyne attached to the adenine ring of NAD can be conjugated via click chemistry to many other functional tags, such as fluorescent tags for in-gel visualization and affinity tags for purification, while its small size will make sure that the NAD analogue will still be accepted by PARPs as

the cosubstrate. We demonstrate that one of the clickable NAD analogues, 6-alkyne-NAD, can be used to label the substrate proteins of PARPs for in-gel visualization and identification. In addition to known PARP-1 substrate proteins, over 70 unknown potential substrate proteins from cell lysate were identified. Among these unknown potential substrate proteins, we demonstrated that four of them are indeed PARP-1 substrates *in vitro*. These results demonstrate that the clickable NAD analogue will be very useful for studying the biological function of PARPs by facilitating the in-gel visualization, isolation, and identification of substrate proteins.

## Results and Discussion

**Labeling of PARP-1 Automodification.** The synthesis of the alkyne-tagged NAD analogues has been reported.<sup>26</sup> Here we tested whether these alkyne-tagged NAD analogues can be accepted by PARPs as a cosubstrate. We first tested the best studied PARP family member, PARP-1. PARP-1 is a 110-kDa protein consisting of three domains: an N-terminal DNA binding domain, a C-terminal catalytic domain, and a central automodification domain. The DNA binding domain can bind to various forms of DNA strand breaks, which stimulate its catalytic activity leading to the poly(ADP-ribosylation) of PARP-1 itself and other target proteins, including histones,<sup>27,28</sup> DEK,<sup>29</sup> and p53.<sup>30–33</sup>

We expressed and purified full-length PARP-1 using baculoviral expression system in Sf-9 cells.<sup>8</sup> The purified protein was incubated with 6-alkyne-NAD and 8-alkyne-NAD in the

- (17) Dynek, J. N.; Smith, S. *Science* **2004**, *304*, 97–100.  
 (18) Chang, P.; Jacobson, M. K.; Mitchison, T. J. *Nature* **2004**, *432*, 645–649.  
 (19) Chang, W.; Dynek, J. N.; Smith, S. *Biochem. J.* **2005**, *391*, 177–184.  
 (20) Chang, P.; Coughlin, M.; Mitchison, T. J. *Nat. Cell Biol.* **2005**, *7*, 1133–1139.  
 (21) Smith, S.; Gariat, I.; Schmitt, A.; de Lange, T. *Science* **1998**, *282*, 1484–1487.  
 (22) Smith, S.; de Lange, T. *Curr. Biol.* **2000**, *10*, 1299–1302.  
 (23) Berwick, D. C.; Tavare, J. M. *Trends Biochem. Sci.* **2004**, *29*, 227–232.  
 (24) Ubersax, J. A.; Woodbury, E. L.; Quang, P. N.; Paraz, M.; Blethrow, J. D.; Shah, K.; et al. *Nature* **2003**, *425*, 859–864.  
 (25) Dani, N.; Stilla, A.; Marchegiani, A.; Tamburro, A.; Till, S.; Ladurner, A. G.; et al. *Proc. Natl. Acad. Sci. U.S.A.* **2009**, *106*, 4243–4248.

- (26) Du, J.; Jiang, H.; Lin, H. *Biochemistry* **2009**, *48*, 2878–2890.  
 (27) Adamietz, P.; Rudolph, A. *J. Biol. Chem.* **1984**, *259*, 6841–6846.  
 (28) Krupitza, G.; Cerutti, P. *Biochemistry* **1989**, *28*, 4054–4060.  
 (29) Gamble, M. J.; Fisher, R. P. *Nat. Struct. Mol. Biol.* **2007**, *14*, 548–555.  
 (30) Kanai, M.; Hanashiro, K.; Kim, S.-H.; Hanai, S.; Boulares, A. H.; Miwa, M.; et al. *Nat. Cell Biol.* **2007**, *9*, 1175–1183.  
 (31) Kanai, M.; Tong, W.-M.; Sugihara, E.; Wang, Z.-Q.; Fukasawa, K.; Miwa, M. *Mol. Cell Biol.* **2003**, *23*, 2451–2462.  
 (32) Simbulan-Rosenthal, C. M.; Rosenthal, D. S.; Luo, R.; Smulson, M. E. *Cancer Res.* **1999**, *59*, 2190–2194.  
 (33) Mendoza-Alvarez, H.; Alvarez-Gonzalez, R. *J. Biol. Chem.* **2001**, *276*, 36425–36430.

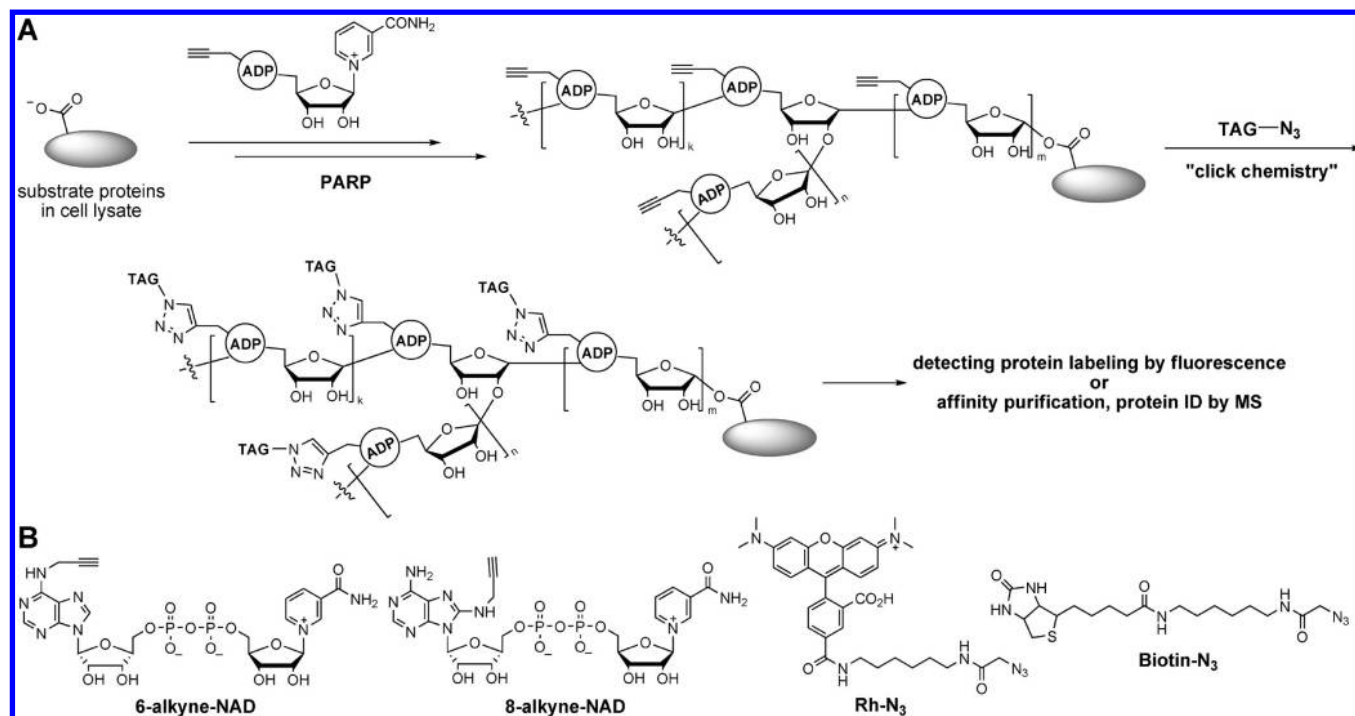


**Figure 2.** (A) Labeling of poly(ADP-ribosylated) proteins with NAD analogues. NAD analogues bearing an alkyne group will be used in PARP-catalyzed reactions. An affinity tag can be added using click chemistry after the substrate protein is labeled. The labeled protein can then be affinity purified, separated on 1D/2D protein gel, and then the sequence identified by MS. (B) Structure of 6-/8-alkyne-NAD, Rh-N<sub>3</sub>, and Biotin-N<sub>3</sub>, which were used in labeling reactions.

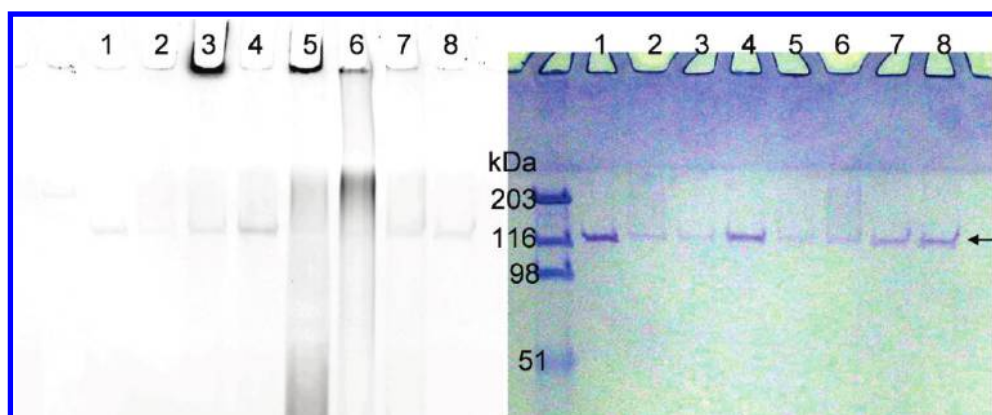


**Figure 3.** Labeling of PARP-1 auto-(ADP-ribosylation) with 6- or 8-alkyne-NAD. The panel on the left shows the image of Rhodamine fluorescence and the panel on the right is the same gel stained with Coomassie Blue. The arrow points at the position of unmodified PARP-1. All lanes contain PARP-1 (0.15  $\mu$ M) and all lanes except 7 and 8 contain ssDNA (0.25  $\mu$ g/ $\mu$ L). Lane 1, control without NAD; lane 2, control with normal NAD (100  $\mu$ M); lane 3, 6-alkyne-NAD (100  $\mu$ M); lane 4, 8-alkyne-NAD (100  $\mu$ M); lane 5, 6-alkyne-NAD (100  $\mu$ M) and NAD (100  $\mu$ M); lane 6, 8-alkyne-NAD (100  $\mu$ M) and NAD (100  $\mu$ M); lane 7, control with 6-alkyne-NAD (100  $\mu$ M), NAD (100  $\mu$ M), and no ssDNA; lane 8, control with 8-alkyne-NAD (100  $\mu$ M), NAD (100  $\mu$ M), and no ssDNA. The fluorescence signal below 116 kDa in lane 5 and 6 is likely due to the hydrolysis of poly(ADP-ribose) chain resulting in poly(ADP-ribose) polymers that are not covalently bound to proteins. The linkage between different ADP-ribose units is a relatively labile ester bond.

presence of salmon sperm DNA (ssDNA), an activator of PARP-1 enzymatic activity. Next, click chemistry was initiated to conjugate the fluorescent tag, Rh-N<sub>3</sub>, to the modified protein. The reaction mixture was then resolved by SDS-PAGE and the fluorescent labeling was detected. The fluorescent image and the corresponding Coomassie Blue-stained gel are shown in Figure 3. With 100  $\mu$ M 6-alkyne-NAD, a strong fluorescent band was observed at the top of the gel (Figure 3, lane 3), suggesting that PARP-1 was extensively poly(ADP-ribosylated). Correspondingly, the intensity of the unmodified PARP-1 band was decreased compared with the control in lane 1. When 100  $\mu$ M NAD was included in the labeling reaction with 6-alkyne-NAD, in addition to the top fluorescent band, a smear of fluorescence

was also observed above the unmodified PARP-1 protein band (Figure 3, lane 5). This smear is likely PARP-1 modified to a lesser degree. A smear of fluorescence signal below 116 kDa was also observed. This is likely due to the hydrolysis of poly(ADP-ribose) chain resulting in poly(ADP-ribose) polymers that are not covalently bound to proteins. The linkage between different ADP-ribose units is a relatively labile ester bond. This result suggests that the presence of normal NAD does not decrease the labeling efficiency with 6-alkyne-NAD and may in fact increase it. This is possibly because 6-alkyne-NAD is not a good substrate for initiation of poly(ADP-ribosylation), but after a poly(ADP-ribose) chain is formed with the better substrate NAD, then 6-alkyne-NAD becomes a better substrate

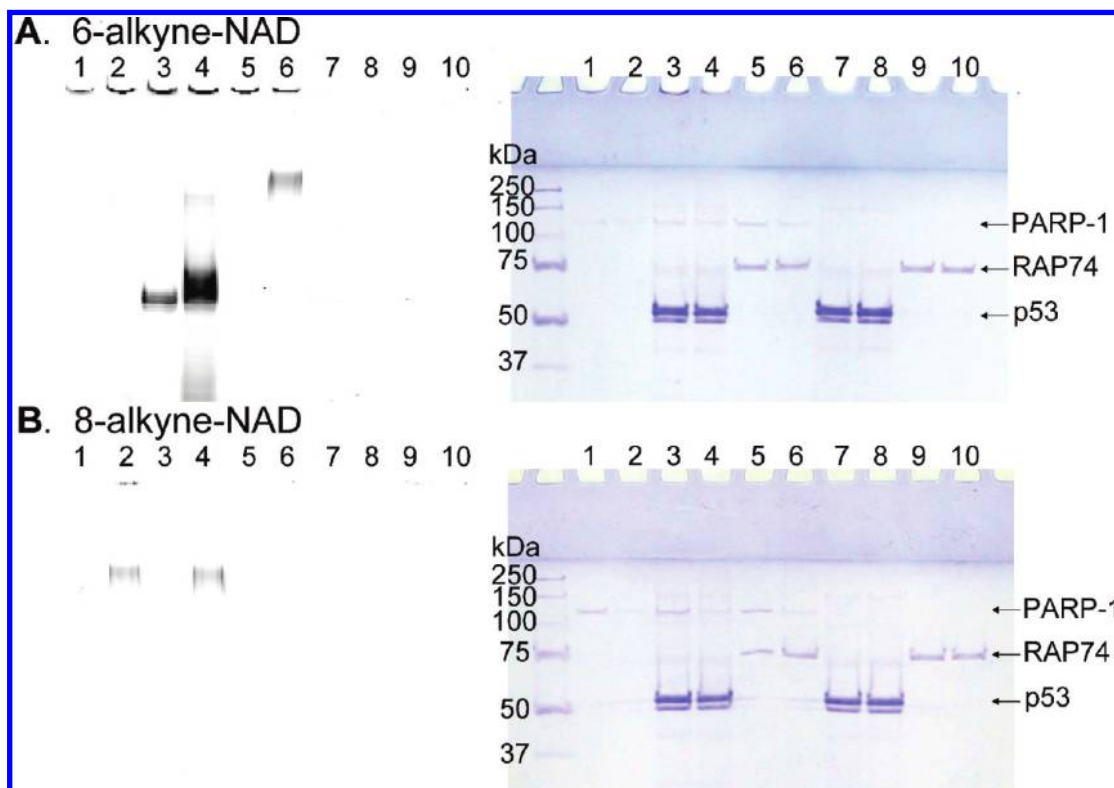


**Figure 4.** Labeling of p53 and RAP74 subunit of TFIIF by PARP-1 using 6-alkyne-NAD (A) and 8-alkyne-NAD (B). The panel on the left shows the image of Rhodamine fluorescence recorded by Typhoon 9400 Variable Mode Imager, and the panel on the right is the same gels stained with Coomassie Blue. In addition to 6- or 8-alkyne-NAD (100  $\mu\text{M}$ ), the following were present in different lanes: 1 and 2, PARP-1 (0.15  $\mu\text{M}$ ); 3 and 4, PARP-1 (0.15  $\mu\text{M}$ ) and p53 (2.8  $\mu\text{M}$ ); 5 and 6, PARP-1 (0.15  $\mu\text{M}$ ) and RAP74 (0.59  $\mu\text{M}$ ); 7 and 8, p53 (2.8  $\mu\text{M}$ ); 9 and 10, RAP74 (0.59  $\mu\text{M}$ ). ssDNA was present in all lanes, and normal NAD (100  $\mu\text{M}$ ) was present in lanes 2, 4, 6, 8, and 10. The fluorescence signal in the loading wells likely came from poly(ADP-ribose)ated PARP-1.

for subsequent elongation of the poly(ADP-ribose) chain, leading to higher labeling efficiency. Without ssDNA (lane 7), the fluorescence signal is comparable to the negative controls (lanes 1 and 2), consistent with the low activity of PARP-1 in the absence of DNA strand breaks. The other analogue, 8-alkyne-NAD, can also label PARP-1 automodification. However, it is less efficient than 6-alkyne-NAD. Even in the presence of normal NAD, the extensive poly(ADP-ribose)ation band at the top of the gel is weak with 8-alkyne-NAD (Figure 3, lane 6). It is possible that attaching the alkyne group at position 8 of the adenine ring produces steric clash when it binds to PARP-1.

To compare the labeling results with clickable NAD analogues to that obtained with  $^{32}\text{P}$ -NAD, we carried out similar labeling experiments with  $^{32}\text{P}$ -NAD (Supporting Information, Figure S1). Comparing the results shown in Figure 3 and Figure S1, the labeling results obtained with 6-alkyne-NAD is very similar to that obtained with  $^{32}\text{P}$ -NAD, particularly when 100  $\mu\text{M}$  normal NAD was present (Figure 3 lane 5 and Figure S1 lane 3). This result suggests that 6-alkyne-NAD can be used to label and detect PARP-1 automodification.

We further demonstrated that two PARP-1 truncations, PARP-1(374–524, the automodification domain) and PARP-1(374–1014, the automodification domain plus the catalytic domain), can be labeled with PARP-1 full-length and 6-alkyne-NAD (Supporting Information, Figure S2). In the presence of 100  $\mu\text{M}$  NAD and 6-alkyne NAD, the labeling of PARP-1(374–1014) reached maximum levels in about 6 min (Supporting Information, Figure S3). The labeling of as little as 2.5 pmol of PARP-1 (374–1014) can be detected (Supporting Information, Figure S4).

**Labeling of Known Substrate Proteins of PARP-1 and Tankyrase-1.** It has been reported that PARP-1 can modify many other proteins,<sup>34</sup> even though the major substrate is PARP-1 itself.<sup>2</sup> To make sure that 6-alkyne-NAD is a robust substrate for PARP-1, we tested whether modification of other substrate proteins can be detected. For this purpose, we chose to use p53 and TFIIF, both of which have previously been reported to be PARP-1 targets.<sup>30–33,35–37</sup> The RAP74 subunit of TFIIF or p53 was incubated with full-length PARP-1 and 6- or 8-alkyne-NAD, followed by click chemistry to conjugate Rh–N<sub>3</sub>. The results shown in Figure 4 demonstrate that p53 can be poly(ADP-ribose)ated by PARP-1 when 6-alkyne-NAD was used, both in the absence and presence of normal NAD (Figure 4A, lanes 3 and 4). The smear over p53 protein band is poly(ADP-ribose)ated p53. The RAP74 subunit of TFIIF can be labeled with 6-alkyne-NAD when normal NAD was present (Figure 4A, lane 6), but not when normal NAD was not present (Figure 4A, lane 5). Comparing lane 6 to lane 2 in Figure 4A, the extra smear on the top is poly(ADP-ribose)ated RAP74. With 8-alkyne-NAD, neither p53 nor RAP74 was labeled (Figure 4B).

To further confirm that 6-alkyne-NAD is a robust substrate for labeling poly(ADP-ribose)ated proteins, we wanted to find out whether substrate proteins of other PARPs can also be

(34) Ogata, N.; Ueda, K.; Kawaichi, M.; Hayaishi, O. *J. Biol. Chem.* **1981**, *256*, 4135–4137.

(35) Kumari, S. R.; Mendoza-Alvarez, H.; Alvarez-Gonzalez, R. *Cancer Res.* **1998**, *58*, 5075–5078.

(36) Simbulan-Rosenthal, C. M.; Rosenthal, D. S.; Luo, R.; Samara, R.; Jung, M.; Dritschilo, A.; et al. *Neoplasia* **2001**, *3*, 179–188.

(37) Rawling, J. M.; Alvarez-Gonzalez, R. *Biochem. J.* **1997**, *324*, 249–253.

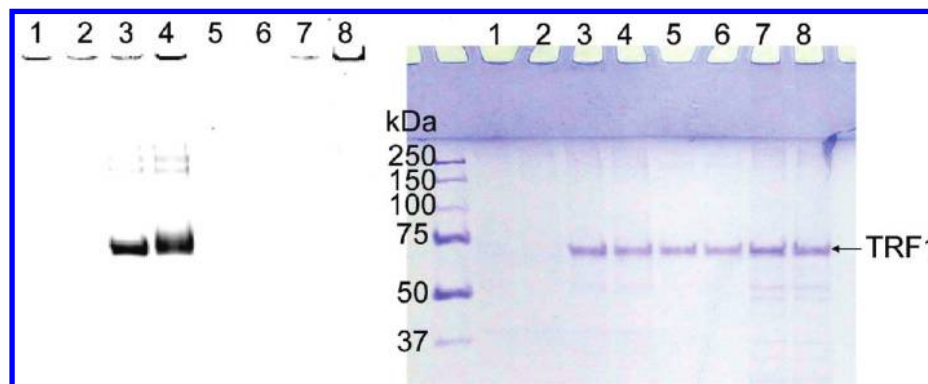


**Figure 5.** Labeling of TRF1 by tankyrase-1 using 6-alkyne-NAD. The panel on the left shows the image of Rhodamine fluorescence, and the panel on the right is the same gel stained with Coomassie Blue. Lanes 1 and 2, tankyrase-1 suspension (0.09  $\mu\text{g}/\mu\text{L}$ ) with 6-alkyne-NAD (100  $\mu\text{M}$ ); 3 and 4, tankyrase-1 suspension (0.09  $\mu\text{g}/\mu\text{L}$ ) and TRF1 (1.1  $\mu\text{M}$ ) with 6-alkyne-NAD (100  $\mu\text{M}$ ); 5 and 6, TRF1 (1.1  $\mu\text{M}$ ) with 6-alkyne-NAD (100  $\mu\text{M}$ ); 7 and 8, suspension of the insoluble fraction of noninfected SF9 cell lysate (0.15  $\mu\text{g}/\mu\text{L}$ , negative control) and TRF1 (1.1  $\mu\text{M}$ ) with 6-alkyne-NAD (100  $\mu\text{M}$ ). Lanes 2, 4, 6, and 8 contained normal NAD (100  $\mu\text{M}$ ).

**Table 1.** Kinetics of PARP-1 and Tankyrase-1 with NAD, 6- and 8-Alkyne-NAD

PARPs	substrates	PARP activity			NADase activity		
		$k_{\text{cat}}$ ( $\text{s}^{-1}$ )	$K_{\text{m}}$ ( $\mu\text{M}$ )	$k_{\text{cat}}/K_{\text{m}}$ ( $\text{s}^{-1} \text{M}^{-1}$ )	$k_{\text{cat}}$ ( $\text{s}^{-1}$ )	$K_{\text{m}}$ ( $\mu\text{M}$ )	$k_{\text{cat}}/K_{\text{m}}$ ( $\text{s}^{-1} \text{M}^{-1}$ )
PARP-1	NAD	$5.2 \pm 0.1$	$97 \pm 7$	$5.4 \times 10^4$	$0.99 \pm 0.06$	$203 \pm 33$	$4.88 \times 10^3$
	6-alkyne-NAD	$0.73 \pm 0.04$	$147 \pm 23$	$5.0 \times 10^3$	$0.94 \pm 0.1$	$1891 \pm 273$	497
	8-alkyne-NAD <sup>a</sup>	N/A	N/A	0.51	N/A	N/A	11.90
Tankyrase-1	NAD	$0.51 \pm 0.04$	$1125 \pm 133$	453	$0.54 \pm 0.02$	$607 \pm 29$	890
	6-alkyne-NAD <sup>a</sup>	N/A	N/A	122	N/A	N/A	252
	8-alkyne-NAD <sup>a</sup>	N/A	N/A	0.29	N/A	N/A	3.41

<sup>a</sup> The reaction rate of PARP-1 or Tankyrase-1 with 6- or 8-alkyne-NAD was linear with the 6- or 8-alkyne-NAD concentration used (10  $\mu\text{M}$  to 1 mM). Thus,  $k_{\text{cat}}$  and  $K_{\text{m}}$  could not be measured and only  $k_{\text{cat}}/K_{\text{m}}$  was obtained.

labeled. For this purpose, we used tankyrase-1, which can regulate telomere length and mitosis by modifying TRF1 and NuMA, respectively. Using the insect cell expression system developed by de Lange and co-workers,<sup>21</sup> we expressed and purified tankyrase-1 and TRF1. The labeling reactions were then carried out, similarly to those above. Consistent with the reported results obtained with <sup>32</sup>P-NAD,<sup>21</sup> we observed efficient TRF1 modification in the presence of tankyrase-1 and 6-alkyne-NAD (Figure 5A, lanes 3 and 4), but not in the absence of tankyrase-1 (Figure 5A, lanes 5–8). These results suggest that 6-alkyne-NAD is a robust substrate, and may be applicable to other PARPs.

**Kinetics of PARP-1 and Tankyrase-1 Labeling with 6-Alkyne-NAD.** To quantify how efficient 6-alkyne-NAD is as a PARP substrate, we measured the steady state kinetics of NAD, 6-alkyne-NAD, and 8-alkyne-NAD in the PARP-1 and Tankyrase-1 automodification reactions. Previously, the kinetics assays were typically done by measuring the PARP-1 automodification using radiolabeled NAD.<sup>38,39</sup> Recently, a chromogenic NAD analogue was also reported.<sup>40</sup> However, both methods cannot be directly applied to the kinetic assay with 6-alkyne-NAD. Thus, we developed a HPLC-based assay to measure the release of nicotinamide. To correct for the NADase activity (hydrolysis of NAD to ADP-ribose and nicotinamide), we also measured the release of ADP-ribose, 6-alkyne-ADP-ribose, or 8-alkyne-ADP-ribose. The  $k_{\text{cat}}$  and  $K_{\text{m}}$  values for the PARP activity and NADase activity are shown in Table 1.

Compared with NAD, the  $k_{\text{cat}}/K_{\text{m}}$  value of 6-alkyne-NAD is 12-fold and 4-fold lower for PARP-1 and Tankyrase-1, respectively. In contrast, 8-alkyne-NAD is a much worse substrate for both PARP-1 and Tankyrase 1, consistent with the labeling results (Figures 3 and 4). Although 6-alkyne-NAD has a lower catalytic efficiency compared with NAD, the labeling efficiency will not be affected significantly because in practice a much higher 6-alkyne-NAD concentration can be used, particularly when comparing to <sup>32</sup>P-NAD, the concentration of which in labeling reactions is limited to a few micromolar by the commercially available <sup>32</sup>P-NAD.

**Identification of Substrate Proteins of PARP-1 Using 6-Alkyne-NAD.** Since 6-alkyne-NAD is a robust substrate for PARP-1, we then tried to use 6-alkyne-NAD to identify substrate proteins of PARP-1 from cell lysate. We used both MCF-7 wild-type and PARP-1 knockdown (KD) cell lysate as the source of the PARP-1 substrate proteins. After the lysate was incubated with 6-alkyne-NAD, click chemistry was used to conjugate the Rh-N<sub>3</sub> fluorescent dye. The fluorescence image shown in Figure 6 suggests that incubation of the cell lysates with PARP-1 and 6-alkyne-NAD indeed led to the poly(ADP-ribosylation) of proteins in the cell lysates.

To identify the proteins that are modified by PARP-1, an affinity tag, Biotin-N<sub>3</sub>, was used for purification and isolation. MCF-7 PARP-1 KD cell lysate was used as the source of the PARP-1 substrate proteins. In the PARP-1 KD cells, because PARP-1 level is decreased (Supporting Information, Figure S5),<sup>41</sup> fewer PARP-1 substrate proteins should be poly(ADP-ribosylated). Thus, more substrate proteins may be available for labeling in the *in vitro* reactions containing recombinant

(38) Kawaichi, M.; Ueda, K.; Hayaishi, O. *J. Biol. Chem.* **1981**, *256*, 9483–9489.

(39) Beneke, S.; Alvarez-Gonzalez, R.; Bürkle, A. *Exp. Gerontol.* **2000**, *35*, 989–1002.

(40) Nottbohm, A. C.; Dothager, R. S.; Putt, K. S.; Hoyt, M. T.; Hergenrother, P. *J. Angew. Chem., Int. Ed.* **2007**, *46*, 2066–2069.

(41) Frizzell, K. M.; Gamble, M. J.; Berrocal, J. G.; Zhang, T.; Krishnakumar, R.; Cen, Y.; et al. *J. Biol. Chem.* **2009**, *284*, 33926–33938.

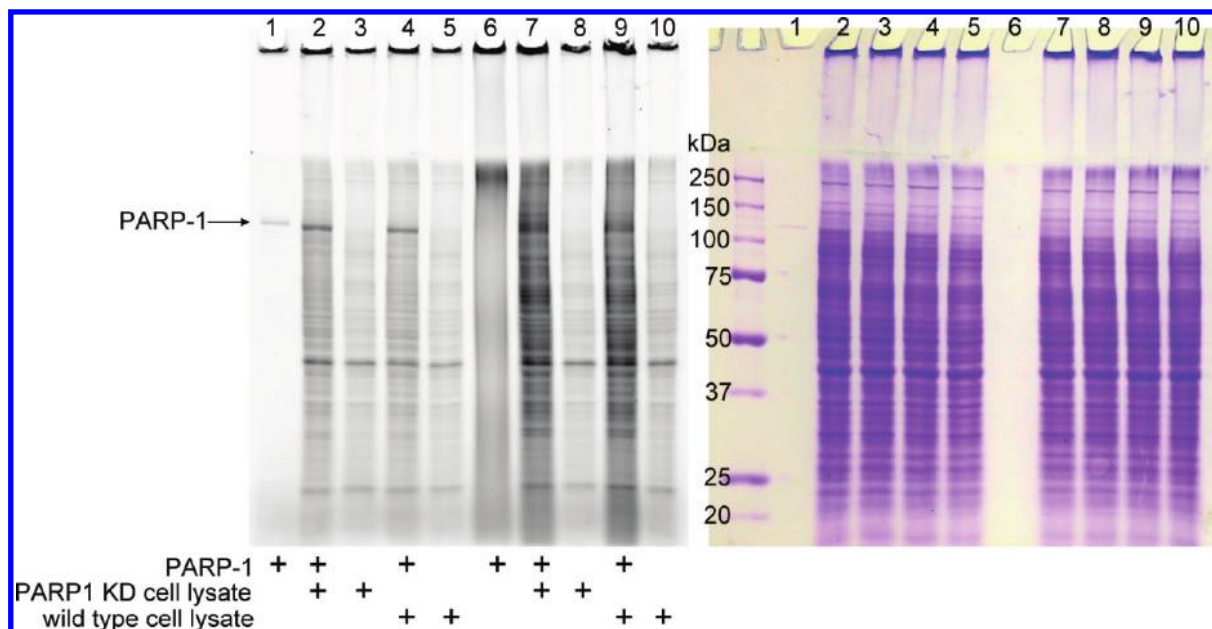


**Figure 6.** Labeling of MCF-7 wild-type and PARP-1 KD cell lysate with PARP-1 and 6-alkyne-NAD. The panel on the left shows the image of Rhodamine fluorescence, and the panel on the right is the same gel stained with Coomassie Blue. PARP-1 (0.075  $\mu\text{M}$ ), MCF-7 wild-type cell lysate (2  $\mu\text{g}/\mu\text{L}$ ) and PARP-1 KD cell lysate (2  $\mu\text{g}/\mu\text{L}$ ) were used in the labeling reactions. All lanes contain 6-alkyne-NAD (100  $\mu\text{M}$ ) and ssDNA (0.25  $\mu\text{g}/\mu\text{L}$ ). Lanes 6–10 contained normal NAD (100  $\mu\text{M}$ ).

PARP-1 and 6-alkyne-NAD. For negative controls, we used 100  $\mu\text{M}$  PJ34 (a PARP-1 inhibitor) or leave out 6-alkyne-NAD in the reactions.

After incubation of PARP-1 and 6-alkyne-NAD with MCF-7 PARP-1 KD cell lysate, click chemistry was carried out to conjugate Biotin- $\text{N}_3$ . Controls were treated similarly. Following the published protocol,<sup>42</sup> labeled proteins were affinity purified and isolated using streptavidin beads, and the samples were prepared and analyzed by nanoLC-MS/MS. It should be noted that proteins from the labeling reactions were denatured and precipitated out with acetone, then solubilized with SDS buffer for affinity purification with streptavidin beads. Under the denaturing conditions, noncovalent interactions between protein–protein or protein–DNA/RNA are minimized, unlike the use of PAR antibodies or macrodomains that use native conditions. Therefore, this affinity purification and identification by nanoLC-MS/MS will give fewer false positive results, making the results more reliable.

About 300 proteins were identified from each sample, including negative controls. A protein is considered a potential substrate proteins if more than 2 peptides are identified in  $\geq 2$  out of 3 samples and it is more abundant in the 3 experimental samples than in the 3 negative controls. The quantification is based on exponentially modified protein abundance index (emPAI) values.<sup>43</sup> Among the  $\sim 300$  proteins identified, 79 proteins with emPAI ratio (emPAI value in experimental sample/emPAI value in negative control) greater than 1.20 were identified as potential PARP-1 substrates (Table S1, Supporting Information). For proteins with emPAI ratios smaller than 2.0, up to three common peptide ions for each protein found in experimental samples and control samples were compared using extracted ion chromatograms.<sup>43</sup> A protein was only considered

a positive hit if the extracted ion chromatograms confirmed that the protein was more abundant in experimental samples than in control samples. The top 45 identified proteins are shown in Table 2. Among the 45 proteins, 6 of them are known substrate proteins of PARP-1, such as PARP-1 (automodification), histones, and heterogeneous nuclear ribonucleoproteins. In addition, 18 of the 45 proteins have been identified as potential poly(ADP-ribosyl)ated proteins in a proteomic study using PAR antibody.<sup>44</sup> These results demonstrate that the strategy of using 6-alkyne-NAD to label and identify PARP-1 substrate proteins works. Not all known substrate proteins of PARP-1 were identified. One possibility is that these proteins have low concentrations in cells and thus are difficult to identify. Alternatively, these proteins may be conditional substrates that can only be poly(ADP-ribosyl)ated under certain cellular conditions.

Among the proteins identified, our attention is drawn to several mitochondrial proteins. Although most known PARP-1 substrates are nuclear proteins, PARP-1's mitochondrial localization has been confirmed recently.<sup>45</sup> This suggests that PARP-1 potentially has more substrate proteins in mitochondria. Consistent with this, several mitochondria proteins have been identified as potential PARP substrates in a recent proteomic study.<sup>46</sup> To further confirm that identified potential substrate proteins are indeed substrates of PARP-1, we chose tubulin and three mitochondrial proteins TRAP1 (TNF receptor-associated protein 1), citrate synthase, and GDH (glutamate dehydrogenase 1) to further validate the results. Tubulin (emPAI ratio 3.86) is a structural protein and was previously identified as a potential PARP substrate.<sup>44</sup> TRAP1 (emPAI ratio 1.32) is a mitochondrial

(44) Gagne, J.-P.; Isabelle, M.; Lo, K. S.; Bourassa, S.; Hendzel, M. J.; Dawson, V. L.; et al. *Nucleic Acids Res.* **2008**, *36*, 6959–6976.

(49) Hassa, P. O.; Hottiger, M. O. *Front. Biosci.* **2008**, *13*, 3046–3082.

(45) Rossi, M. N.; Carbone, M.; Mostocotto, C.; Mancone, C.; Tripodi, M.; Maione, R.; et al. *J. Biol. Chem.* **2009**, *284*, 31616–31624.

(46) Lai, Y.; Chen, Y.; Watkins, S. C.; Nathaniel, P. D.; Guo, F.; Kochanek, P. M.; et al. *J. Neurochem.* **2008**, *104*, 1700–1711.

(42) Weerapana, E.; Speers, A. E.; Cravatt, B. F. *Nat. Protoc.* **2007**, *2*, 1414–1425.

(43) Schulze, W. X.; Usadel, B. *Annu. Rev. Plant Biol.* **2010**, *61*, 491–516.

**Table 2.** Potential Substrate Proteins of PARP-1 Identified from MS Using the Labeling Strategy with 6-Alkyne-NAD<sup>a</sup>

protein accession name	description	MW (Da)	known substrates of PARP-1	potential PARP substrates identified in other proteomic studies
ATP5L_HUMAN	ATP synthase subunit g	11421		
BAP31_HUMAN	B-cell receptor-associated protein 31	28031		
CH10_HUMAN	10 kDa heat shock protein	10925		
COX41_HUMAN	Cytochrome c oxidase subunit 4 isoform 1	19621		
DDX17_HUMAN	Probable ATP-dependent RNA helicase DDX17	72953		reported in ref 44
DDX5_HUMAN	Probable ATP-dependent RNA helicase DDX5	69618		reported in ref 44
DHE3_HUMAN	Glutamate dehydrogenase 1	61701		reported in ref 44
EF1G_HUMAN	Elongation factor 1-gamma	50429		
ETFA_HUMAN	Electron transfer flavoprotein subunit alpha	35400		
FUBP2_HUMAN	Far upstream element-binding protein 2	73443		
FUS_HUMAN	RNA-binding protein FUS	53622		
GLYM_HUMAN	Serine hydroxymethyltransferase	56414		
GSTK1_HUMAN	Glutathione S-transferase kappa 1	25594		
H2B1C_HUMAN	Histone H2B type 1-C/E/F/G/I	13811	reviewed in ref 49	
H31T_HUMAN	Histone H3.1t	15613	reviewed in ref 49	
HNRPL_HUMAN	Heterogeneous nuclear ribonucleoprotein L	64720		reported in ref 44
HNRPM_HUMAN	Heterogeneous nuclear ribonucleoprotein M	77749	reviewed in ref 49	
HP1B3_HUMAN	Heterochromatin protein 1-binding protein 3	61454		
HXK1_HUMAN	Hexokinase-1	103561		reported in ref 44
IDH3A_HUMAN	Isocitrate dehydrogenase [NAD] subunit alpha	40022		
IDHP_HUMAN	Isocitrate dehydrogenase [NADP]	51333		
IMB1_HUMAN	Importin subunit beta-1	98420		reported in ref 44
KU70_HUMAN	ATP-dependent DNA helicase 2 subunit 1	70084	reviewed in ref 49	
LETM1_HUMAN	LETM1 and EF-hand domain-containing protein 1	83986		
MATR3_HUMAN	Matrin-3	95078		reported in ref 44
MPCP_HUMAN	Phosphate carrier protein	40525		reported in ref 44
NPM_HUMAN	Nucleophosmin	32726	reviewed in ref 49	
PARP1_HUMAN	Poly [ADP-ribose] polymerase 1	113811	reviewed in ref 49	
PHB_HUMAN	Prohibitin	29843		reported in ref 44
QCR2_HUMAN	Cytochrome b-c1 complex subunit 2	48584		reported in ref 44
RBM39_HUMAN	RNA-binding protein 39	59628		
RL19_HUMAN	60S ribosomal protein L19	23565		reported in ref 44
RL26L_HUMAN	60S ribosomal protein L26-like 1	17246		reported in ref 44
RL7_HUMAN	60S ribosomal protein L7	29264		reported in ref 44
RS14_HUMAN	40S ribosomal protein S14	16434		reported in ref 44
RS2_HUMAN	40S ribosomal protein S2	31590		reported in ref 44
RS24_HUMAN	40S ribosomal protein S24	15413		reported in ref 44
RS3_HUMAN	40S ribosomal protein S3	26842		
SFRS1_HUMAN	Splicing factor, arginine/serine-rich 1	27842		reported in ref 44
SFRS6_HUMAN	Splicing factor, arginine/serine-rich 6	39677		
SFRS7_HUMAN	Splicing factor, arginine/serine-rich 7	27578		
TBB2C_HUMAN	Tubulin beta-2C chain	50255		reported in ref 44
TMED9_HUMAN	Transmembrane emp24 domain-containing protein 9	27374		
TR150_HUMAN	Thyroid hormone receptor-associated protein 3	108658		
UBIQ_HUMAN	Ubiquitin	8560		

<sup>a</sup> Top 45 potential substrate proteins of PARP-1 (emPAI ratio >1.50) were listed. References are given for known substrate proteins of PARP-1 and potential PARP substrate proteins identified in other proteomic studies. Full list of identified potential substrate proteins of PARP-1 is given in Supporting Information.

heat shock protein 75 with antioxidant and antiapoptotic functions.<sup>47</sup> It has been shown to protect cells from apoptosis induced by DNA damaging reagents. GDH (emPAI ratio 2.47) catalyzed the conversion of glutamate to  $\alpha$ -ketoglutarate, which feeds into the tricarboxylic acid (TCA) cycle for energy production. Citrate synthase (emPAI ratio 1.25) is an enzyme in the TCA cycle. Tubulin and GDH were both identified in a previous proteomic studies as potential PARP substrates but they have not been confirmed in *in vitro* enzyme assays.<sup>44</sup> TRAP1 and citrate synthase have not been known to be PARP-1 substrates. TRAP1 can be expressed recombinantly,<sup>48</sup> while GDH, citrate synthase, and tubulin are commercially available. Thus, we tested whether these proteins can be poly(ADP-ribosyl)ated by PARP-1 *in vitro* using 6-alkyne-NAD. Comparing lanes 3 and 4 with lanes 1 and 2 (Figure 7), it is clear that all

four proteins were poly(ADP-ribosyl)ated by PARP-1 when normal NAD was present. GDH was modified even when no normal NAD was present. These results further confirm that the proteins we identified as PARP-1 substrates should be highly reliable. Thus, the strategy of labeling, isolating, and identifying PARP-1 substrate proteins with 6-alkyne-NAD is successful. The substrate proteins that we identified for PARP-1 should be very useful for understanding the biological function of PARP-1 and the strategy should be similarly applicable to other PARPs.

## Conclusions

We have demonstrated that the clickable 6-alkyne-NAD is an efficient substrate that can be used to label poly(ADP-ribosyl)ated proteins. In contrast, 8-alkyne-NAD is not an efficient substrate for PARPs. Using the alkyne functional group,

(47) Landriscina, M.; Amoroso, M. R.; Piscazzi, A.; Esposito, F. *Gynecol. Oncol.* **2010**, *117*, 177–182.

(48) Felts, S. J.; Owen, B. A. L.; Nguyen, P.; Trepel, J.; Donner, D. B.; Toft, D. O. *J. Biol. Chem.* **2000**, *275*, 3305–3312.

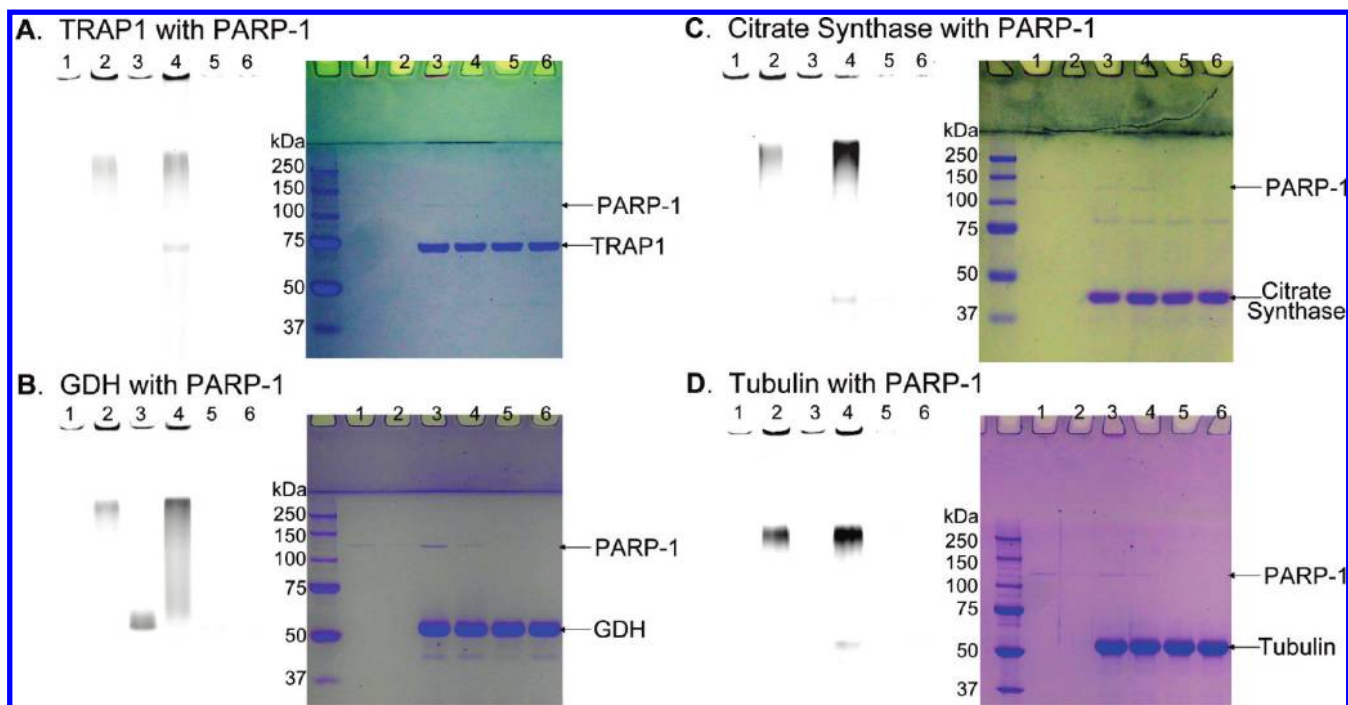


**Figure 7.** Labeling of TRAP1 (A), GDH (B), citrate synthase (C), and tubulin (D) by PARP-1 using 6-alkyne-NAD. The panel on the left shows the image of Rhodamine fluorescence, and the panel on the right is the same gels stained with Coomassie Blue. All lanes contain 6-alkyne-NAD (100  $\mu\text{M}$ ) and ssDNA (0.25  $\mu\text{g}/\mu\text{L}$ ). Lanes 1 and 2, PARP-1 (0.05  $\mu\text{M}$ ); 3 and 4, PARP-1 (0.05  $\mu\text{M}$ ) with TRAP1 (1.0  $\mu\text{M}$ , A) or GDH (3.1  $\mu\text{M}$ , B) or citrate synthase (3.37  $\mu\text{M}$ , C) or tubulin (3.64  $\mu\text{M}$ , D); 5 and 6, TRAP1 (1.0  $\mu\text{M}$ , A), GDH (3.1  $\mu\text{M}$ , B), citrate synthase (3.37  $\mu\text{M}$ , C), or tubulin (3.64  $\mu\text{M}$ , D). Lanes 2, 4, and 6 contained normal NAD (100  $\mu\text{M}$ ).

fluorescent or affinity tags can be conveniently installed on the substrate proteins to facilitate in-gel visualization and identification of the substrate proteins. Over 70 potential novel substrate proteins of PARP-1 have been identified using the labeling strategy with 6-alkyne-NAD, including many mitochondrial proteins. Tubulin, TRAP1, citrate synthase, and GDH were further proved to be PARP-1 substrate proteins *in vitro*. We believe 6-alkyne-NAD will greatly facilitate the identification of the substrate proteins of the 17 PARPs in humans and help to understand their biological functions.

### Experimental Section

**General Methods.** Reagents were obtained from Aldrich in the highest purity available and used as supplied. Kinetics experiments were carried out on a SHIMADZU LCMS-QP8000 $\alpha$  with a Sprite TARGA C18 column (40  $\times$  2.1 mm, 5  $\mu\text{m}$ , Higgins Analytical, Inc.) monitoring at 260 nm. Solvents were 50 mM ammonium acetate pH 5.4 (buffer A) and 50% methanol in water (buffer B). Rhodamine fluorescence signal from protein gel was recorded by Typhoon 9400 Variable Mode Imager (GE Healthcare Life Sciences) with setting of Green (532 nm)/555BP20 PMT450 V (normal sensitivity), and analyzed by ImageQuant TL v2005. The syntheses of 6-alkyne-NAD, 8-alkyne-NAD, Rh-N<sub>3</sub>, and *N*-(6-aminohexyl)-azidoacetamide (for synthesis of Biotin-N<sub>3</sub>) have been reported.<sup>26,50</sup> The synthesis of Biotin-N<sub>3</sub> is given in the Supporting Information. ssDNA was purchased from Sigma and used after sonication. RAP74 (one subunit of TFIIIF) was purchased from ProteinOne (Bethesda, MD). GDH (from bovine liver, type II) and citrate synthase (from porcine heart) were purchased from Sigma. Tubulin (from bovine brain) was purchased from Cytoskeleton (Denver, CO).

**Expression of PARP-1 Full-Length and Truncations.** FLAG-tagged human PARP-1 (PARP-1-FLAG) was purified from SF9

insect cells by FLAG M2 affinity chromatography following published procedures.<sup>8</sup> The PARP-1 truncation (374–524) was PCR-amplified using primers 5'-CACCGCCTCGGCTCCTGCTGCT-3' and 5'-TTATTTTCATTCTCTTTTCAGATTGTT-3'. The PARP-1 truncation (374–1014) was PCR-amplified using primers 5'-CACCGCCTCGGCTCCTGCTGCT-3' and 5'-TTACCACAGG-GAGGCTCTAAAAT-3'. Amplified products were cloned using TOPO and Gateway cloning technology (Invitrogen Corporation, Carlsbad, CA) into pDEST-F1 (PARP-1(374–1014)) and pDEST-566 (PARP-1(374–524)) for expression. PARP-1 (374–524) and PARP-1 (374–1014) were expressed in *Escherichia coli* BL21 pRARE2 strain. Cells were first cultured in LB media at 37  $^{\circ}\text{C}$  and 200 rpm to OD<sub>600</sub>  $\sim$ 0.5 in MaxQ 5000 shaker (Barnstead International, Dubuque, IA). The temperature was then changed to 15  $^{\circ}\text{C}$  and the expression was induced by adding isopropyl  $\beta$ -D-thiogalactoside (IPTG) to 0.1 mM. After incubation at 15  $^{\circ}\text{C}$  for 24 h, cells were harvested by centrifugation at 6370g for 10 min. After resuspended in lysis buffer (20 mM Tris-HCl, 500 mM NaCl, 30 mM imidazole, pH 8.0) at 4  $^{\circ}\text{C}$ , cells were lysed using an EmulsiFlex-C3 cell disruptor (AVESTIN, Inc., Canada), and cell lysate was clarified by centrifugation at 48 400g for 30 min at 4  $^{\circ}\text{C}$ . Protein was purified by Bio-Rad BioLogic DuoFlow FPLC using a HisTrap HP 5 mL column (GE Healthcare) with a linear gradient of imidazole from 30 to 500 mM in elution buffer (20 mM Tris-HCl, 500 mM NaCl, pH 8.0). Fractions containing PARP-1 proteins were collected and dialyzed to 25 mM Tris, pH 6.0, 50 mM NaCl (for PARP-1 (374–1014)) or to 25 mM Tris, pH 8.0, 50 mM NaCl, 1 mM DTT (for PARP-1 (374–524)) at 4  $^{\circ}\text{C}$ . Protein concentrations were determined by Bradford assay or by comparing Coomassie brilliant blue staining with BSA standards after SDS-PAGE.

**Expression of p53.** GST-tagged human p53 in pGEX-2T vector was transformed into *E. coli* BL21 pRARE2 strain. Cells were first cultured in LB media at 37  $^{\circ}\text{C}$  and 200 rpm to OD<sub>600</sub>  $\sim$ 0.5. The temperature was then changed to 15  $^{\circ}\text{C}$  and the expression was induced by adding isopropyl  $\beta$ -D-thiogalactoside (IPTG) to 0.1 mM. After incubation at 15  $^{\circ}\text{C}$  for 24 h, cells were harvested by

(50) Jiang, H.; Congleton, J.; Liu, Q.; Merchant, P.; Malavasi, F.; Lee, H. C.; et al. *J. Am. Chem. Soc.* **2009**, *131*, 1658–1659.

centrifugation at 6370g for 10 min. Cells were resuspended in GST binding buffer (4.3 mM Na<sub>3</sub>PO<sub>4</sub>, 1.47 mM K<sub>3</sub>PO<sub>4</sub>, 137 mM NaCl, 2.7 mM KCl, pH 7.3) at 4 °C, and lysed by using an EmulsiFlex-C3 cell disruptor. Cell lysate was clarified by centrifugation at 48 400g for 30 min at 4 °C, and incubated with 1 mL of GST-Bind Resin (Novagen) for 1 h at 4 °C. The resin was washed with GST binding buffer thoroughly, and then incubated with 150 units Thrombin (GE Healthcare) for 12 h at 4 °C. The supernatant was collected and protein was dialyzed into 25 mM Tris-HCl, pH 8.0, 50 mM NaCl, and 1 mM DTT at 4 °C.

**Expression of Tankyrase-1 and TRF1.** His-tagged human tankyrase-1 and TRF1 in baculovirus vector were provided from Dr. de Lange, and proteins were purified from SF9 insect cells following the published procedure.<sup>21</sup> Recombinant tankyrase-1 was found in the insoluble fraction during the purification. However, the suspension of insoluble fractions contains active tankyrase-1 and was used in the labeling reactions. The suspension of insoluble fraction from noninfected SF9 cells was used as the negative control.

**Automodification of PARP-1 with 6- or 8-Alkyne-NAD.** PARP-1 (0.15 μM), ssDNA (0.25 μg/μL), and 6- or 8-alkyne-NAD (100 μM) with or without NAD (100 μM) in 10 μL reaction buffer (50 mM Tris-HCl, 4 mM MgCl<sub>2</sub>, 0.2 mM DTT, pH 8.0) were incubated at 37 °C for 30 min. Control experiments were done without ssDNA. Then, the click chemistry step was carried out (described later).

**Labeling of p53 and RAP74 by PARP-1 with 6- or 8-Alkyne-NAD.** PARP-1 (0.15 μM), p53 (2.8 μM) or RAP74 (0.59 μM), ssDNA (0.25 μg/μL), and 6- or 8-alkyne-NAD (100 μM) with or without NAD (100 μM) in 10 μL reaction buffer were incubated at 37 °C for 30 min (without NAD) or 6 min (with NAD). Shorter incubation time was used because if longer incubation time is used, the protein will be extensively poly(ADP-ribosylated) and cannot be distinguished from the automodified PARP-1. Control experiments were done without PARP-1 or p53 or RAP74. Then, the click chemistry step was carried out.

**Labeling of TRAP1, GDH, Citrate Synthase, And Tubulin by PARP-1 with 6-NAD.** PARP-1 (0.05 μM), TRAP1 (1.0 μM, overexpressed and purified according to published procedures<sup>48</sup>), GDH (3.1 μM), citrate synthase (3.37 μM), tubulin (3.64 μM), ssDNA (0.25 μg/μL), and 6-alkyne-NAD (100 μM) with or without NAD (100 μM) in 10 μL reaction buffer were incubated at 37 °C for 30 min (without NAD) or 6 min (with NAD). Control experiments were done without PARP-1 or without TRAP1, GDH, citrate synthase, or tubulin. Then, the click chemistry step was carried out.

**Labeling of TRF1 by Tankyrase-1 with 6- or 8-Alkyne-NAD.** Tankyrase-1 pellet suspension (0.09 μg/μL) or noninfected SF9 cell pellet suspension (0.15 μg/μL), TRF1 (1.1 μM), and 6- or 8-alkyne-NAD (100 μM) with or without NAD (100 μM) in 10 μL reaction buffer were incubated at 37 °C for 30 min. Control experiments were done without tankyrase-1 or TRF1. Then, the click chemistry step was carried out.

**Click Chemistry Condition to Conjugate Rh-N<sub>3</sub> and Detection of Poly(ADP-ribosylation) by Fluorescence.** Rh-N<sub>3</sub> (in DMF) was added to the above labeling reactions to a final concentration of 200 μM, followed by the addition of Tris[(1-benzyl-1*H*-1,2,3-triazol-4-yl)methyl]amine<sup>51</sup> (in DMF, final concentration 600 μM), CuSO<sub>4</sub> (in water, final concentration 1 mM), and TCEP (in water, final concentration 1 mM).<sup>52</sup> After the click chemistry was allowed to proceed at room temperature for 15 min, the reaction mixture was mixed with 10 μL of 2× protein loading buffer and heated at 100 °C for 6 min. The samples were then resolved by SDS-PAGE using 12% acrylamide gel. Before staining with Coomassie blue, the fluorescence image of the gel was

recorded by Typhoon 9400 imager. The image of protein gel after Coomassie blue staining was recorded with a digital camera (Canon PowerShot S3).

**Kinetics of PARP-1 with NAD, 6-Alkyne-NAD, and 8-Alkyne-NAD as Substrates.** PARP-1 (0.065 μM), ssDNA (0.05 μg/μL) with different concentrations of NAD, 6-alkyne-NAD, or 8-alkyne-NAD (from 10 μM to 1 mM) in 30 μL reactions (50 mM Tris-HCl, 4 mM MgCl<sub>2</sub>, pH 8.0) were incubated at 25 °C for 1 min (with NAD), 15 min (with 6-alkyne-NAD), or 60 min (with 8-alkyne-NAD). The reactions were quenched with 1 M HClO<sub>4</sub>, and then neutralized with 3 M K<sub>2</sub>CO<sub>3</sub> 5 min later. After centrifugation, the supernatant was analyzed by a SHIMADZU LCMS-QP8000α with a Sprite TARGA C18 column (40 × 2.1 mm, 5 μm, Higgins Analytical, Inc.) monitoring at 260 nm. Solvents were 50 mM ammonium acetate pH 5.4 (buffer A) and 50% methanol in water (buffer B). For PARP-1 with NAD reactions, compounds were eluted at a flow rate of 0.3 mL/min with 0% solvent B for 1 min, followed by a linear gradient of 0–3% solvent B over 14 min, and back to 0% solvent B over 2 min. Retention times of ADP-ribose, nicotinamide and NAD were 1.89, 3.52, and 8.01 min, respectively. For PARP-1 with 6-alkyne-NAD or 8-alkyne-NAD reactions, compounds were eluted at a flow rate of 0.3 mL/min with 0% solvent B for 1 min, followed by a linear gradient of 0–1% solvent B over 5 min, then 1–50% solvent B over 5 min, and finally 50% solvent B for 1 min before equilibrating the column back to 0% solvent B over 2 min. Retention times of nicotinamide, 6-alkyne-ADP-ribose, 8-alkyne-ADP-ribose, 6-alkyne-NAD, and 8-alkyne-NAD were 3.52, 8.42, 6.98, 10.59, and 10.65 min, respectively. Reaction progress was monitored by the formation of nicotinamide, ADP-ribose, 6-alkyne-ADP-ribose, and 8-alkyne-ADP-ribose. The quantification of nicotinamide, ADP-ribose, 6-alkyne-ADP-ribose, and 8-alkyne-ADP-ribose produced in the reaction was analyzed by the integration of absorption peak monitored at 260 nm comparing with the plot of nicotinamide, ADP-ribose, 6-alkyne-ADP-ribose, and 8-alkyne-ADP-ribose standards. The *k*<sub>cat</sub> and *K*<sub>m</sub> values were obtained by curve-fitting the *V*[*E*] ~ [*S*] plot by KaleidaGraph. NADase activity was obtained from the formation of ADP-ribose, 6-alkyne-ADP-ribose, and 8-alkyne-ADP-ribose. PARP activity was obtained from the formation of nicotinamide after deduction of ADP-ribose, 6-alkyne-ADP-ribose, and 8-alkyne-ADP-ribose.

**Kinetics of Tankyrase-1 with NAD, 6-alkyne-NAD, and 8-alkyne-NAD as Substrates.** Tankyrase-1 (0.03 μM) with different concentrations of NAD, 6-alkyne-NAD, or 8-alkyne-NAD (from 10 μM to 1 mM) in 30 μL reactions (50 mM Tris-HCl, 4 mM MgCl<sub>2</sub>, pH 8.0) were incubated at 25 °C for 30 min (with NAD), 2 h (with 6-alkyne-NAD), or 13 h (with 8-alkyne-NAD). Then, the reactions were quenched and handled same as PARP-1 reactions for kinetics. NADase and PARP activities of tankyrase-1 were measured same as PARP-1 kinetics.

**Cell Lysate of MCF-7 Wild-Type and PARP-1 KD Cells.** MCF-7 wild-type and PARP-1 KD cells<sup>41</sup> from 10 10-cm plates (90% confluency) were lysed by Dounce Homogenizer in 5 mL of lysis buffer (25 mM Tris, 50 mM NaCl, 10% glycerol, pH 7.4) with 100 μL of protease inhibitor cocktail (Sigma, Saint Louis, MO). The cell lysate was then centrifuged at 2000g for 15 min at 4 °C. Under this condition, the pellet contained nuclei, mitochondria, and other organelles. The pellet was solubilized in 4 mL of lysis buffer with 1% NP-40 and 100 μL of protease inhibitor cocktail. After centrifugation at 14 000g for 5 min at 4 °C, the supernatant was collected as cell lysate for later labeling reactions with PARP-1 and 6-alkyne-NAD.

**Labeling of MCF-7 Wild-Type and PARP-1 KD Cell Lysate by PARP-1 with 6-Alkyne-NAD.** PARP-1 (0.075 μM), MCF-7 wild-type cell lysate (2 μg/μL), or PARP-1 KD cell lysate (2 μg/μL), ssDNA (0.25 μg/μL), and 6-alkyne-NAD (100 μM) with or without NAD (100 μM) in 10 μL of reaction buffer with 0.5% NP-40 were incubated at 37 °C for 30 min. Control experiments

(51) Wang, Q.; Chan, T. R.; Hilgraf, R.; Fokin, V. V.; Sharpless, K. B.; Finn, M. G. *J. Am. Chem. Soc.* **2003**, *125*, 3192–3193.

(52) Rostovtsev, V. V.; Green, L. G.; Fokin, V. V.; Sharpless, K. B. *Angew. Chem., Int. Ed.* **2002**, *41*, 2596–2599.

were done without PARP-1 or without cell lysates. Then, the click chemistry step was carried out.

**Pull-down of Substrate Proteins of PARP-1 Using 6-Alkyne-NAD.** Cell lysate of MCF-7 PARP-1 KD cells (2 mg) was incubated with PARP-1 (1.8  $\mu\text{g}$ ), 6-alkyne-NAD (10 nmol, final concentration 10  $\mu\text{M}$ ), and ssDNA (20  $\mu\text{g}$ ) in 1 mL of reaction buffer at 37 °C for 30 min with gentle rotating. Control experiments were done with 100  $\mu\text{M}$  PJ34 (a PARP-1 inhibitor) or without 6-alkyne-NAD. Then, the click chemistry step was carried out with Biotin-N<sub>3</sub> (in DMF, final concentration 16  $\mu\text{M}$ ), Tris[(1-benzyl-1H-1,2,3-triazol-4-yl)methyl]amine (in DMF, final concentration 200  $\mu\text{M}$ ), CuSO<sub>4</sub> (in water, final concentration 800  $\mu\text{M}$ ), and TCEP (in water, final concentration 800  $\mu\text{M}$ ) at room temperature for 30 min. The reaction mixture was denatured and precipitated with 10 mL of cold acetone. After centrifugation at 14 000g for 5 min at 4 °C, the precipitate was further washed with 3  $\times$  1 mL of cold methanol to remove extra small molecule reagents. After solubilizing the precipitate in 1 mL of 2% SDS in PBS with heating at 90 °C for 10 min and centrifugation at 14 000g for 5 min at room temperature, the supernatant was diluted to 10 mL by adding 9 mL of PBS (final 0.2% SDS in PBS), and incubated with 100  $\mu\text{L}$  of streptavidin beads (Pierce Biotechnology, Rockford, IL) for 90 min at room temperature with gentle rotating. After centrifugation at 1000g for 2 min at room temperature, the beads were further washed with 3  $\times$  1 mL 0.2% SDS in PBS, 3  $\times$  1 mL PBS, 3  $\times$  1 mL (20 mM Tris, 500 mM KCl, pH 7.4), 3  $\times$  1 mL (20 mM Tris, pH 7.4), and then incubated with 400  $\mu\text{L}$  of 6 M urea in PBS with 9.5 mM TCEP for 20 min at 35 °C with gentle rotating. Iodoacetamide (20  $\mu\text{L}$  400 mM in water) was added to the suspension of beads with further incubation for 20 min at 35 °C with gentle rotating. After dilution with 760  $\mu\text{L}$  of PBS and removal of supernatant, the beads were incubated with 2  $\mu\text{g}$  of Trypsin (Promega, Madison, WI) in 200  $\mu\text{L}$  of 2 M urea in PBS and 1 mM CaCl<sub>2</sub> at 37 °C for 8 h with gently rotating. The supernatant was collected and combined with washings of 2  $\times$  300  $\mu\text{L}$  water from beads. Then, the digested peptides in above solution were purified with Sep-Pak Vac C18 cartridge (Waters Corporation, Milford, MA) and analyzed by nanoLC-MS/MS. Each experiment was done individually three times. Proteins identified in the samples but not in the control experiments were listed in Table 2.

**Protein Identification by NanoLC/MS/MS Analyses.** The tryptic digest was reconstituted in 10  $\mu\text{L}$  of 2% acetonitrile (ACN) with 0.5% formic acid (FA) for nanoLC-ESI-MS/MS analysis, which is carried out using a LTQ-Orbitrap Velos (Thermo-Fisher Scientific, San Jose, CA) mass spectrometer equipped with nano ion source. The Orbitrap is interfaced with an UltiMate3000 MDLC system (Dionex, Sunnyvale, CA). The nanoLC was carried out by Dionex UltiMate3000 MDLC system (Dionex, Sunnyvale, CA). An aliquot of tryptic peptide (3.0  $\mu\text{L}$ ) was injected onto a PepMap C18 trap column (5  $\mu\text{m}$ , 300  $\mu\text{m}$   $\times$  5 mm, Dionex) at 20  $\mu\text{L}/\text{min}$  flow rate for online desalting and then separated on a PepMap C-18 RP nano column (3  $\mu\text{m}$ , 75  $\mu\text{m}$   $\times$  15 cm), and eluted in a 90 min gradient of 5–38% ACN in 0.1% FA at 300 nL/min., followed by a 3-min ramping to 95% ACN–0.1% FA and a 5-min holding at 95% ACN–0.1% FA. The column was re-equilibrated with 2% ACN–0.1% FA for 20 min prior to the next run. The eluted peptides are detected by Orbitrap through nano ion source containing a 10- $\mu\text{m}$  analyte emitter (NewObjective, Woburn, MA). The Orbitrap Velos is operated in positive ion mode with nano spray voltage set at 1.5 kV and source temperature at 175 °C. Either internal calibration using the background ion signal at  $m/z$  445.120025 as a lock mass or external calibration for FT mass analyzer is performed. The instrument is performed at parallel data-

dependent acquisition (DDA) mode using FT mass analyzer for one survey MS scan for precursor ions followed by MS/MS scans on top 7 most intensive peaks with multiple charged ions above a threshold ion count of 5000 in LTQ mass analyzer. MS survey scans at a resolution of 60 000 (fwhm at  $m/z$  400), for the mass range of  $m/z$  375–1400. Dynamic exclusion parameters were set at repeat count 1 with a 20 s repeat duration, exclusion list size of 500, 30 s exclusion duration, and  $\pm$ 10 ppm exclusion mass width. Collision induced dissociation (CID) parameters were set at the following values: isolation width 2.0  $m/z$ , normalized collision energy 35%, activation  $Q$  at 0.25, and activation time 30 ms. All data are acquired under Xcalibur 2.1 operation software (Thermo-Fisher Scientific).

**Data Analysis.** All MS and MS/MS raw spectra were processed using Proteome Discoverer 1.1 (PD1.1, Thermo) and the spectra from each DDA file are output as an MGF file for subsequent database search using in-house license Mascot Deamon (version 2.2.04, Matrix Science, Boston, MA). The *human* protein sequence database containing 20 349 sequence entries in the Swiss-Prot database downloaded on January 21, 2010 was used for database search and the search was performed to query to Swiss-Prot database (taxonomy: human) with one missed cleavage site by trypsin allowed. The peptide tolerance was set to 10 ppm and MS/MS tolerance was set to 0.8 Da. A fixed carbamidomethyl modification of cysteine, variable modifications on methionine oxidation and deamidation of asparagine and glutamine were set. Data filtering parameters were as follows: (a) the peptide identity probability is 99.9%CI with 35 peptide score cutoff; (b) only top matching proteins with  $p < 0.001$  (expectation value) were considered in the analysis, and (c) at least two distinct peptides met above criteria hit for each proteins as a finally identified protein list and used for obtaining exponentially modified protein abundance index (emPAI) number for each identified proteins. After filtering, the emPAIs outputted directly from Mascot results for each identified proteins were used for estimation of relative protein abundance in three experimental samples versus the three negative control samples. A protein is considered a potential PARP-1 substrate only if the emPAI ratio (experimental/control) is more than 1.20. If the emPAI ration is between 2.0 and 1.20, the emPAI-based relative protein quantification results were also manually validated by averaging precursor ion peak areas of up to three top score peptides (found in both experimental samples and control samples) for each protein using extracted ion chromatograms in PD1.1 software.

**Acknowledgment.** H.J. and H.L. thank Donald Ruhl and Joanna Berrocal for help with protein expression in Sf9 cells. We thank Dr. Jun-Lin Guan (University of Michigan Medical School) for providing the p53 expression vector, Dr. Titia de Lange (Rockefeller University) for providing the Sf9 expression cells for Tankyrase-1 and TRF-1. This work is supported in part by Dreyfus Foundation (New Faculty Award to H.L.), NIH R01 GM086703 (H.L.), and NIH R01 DK069710 (W.L.K.).

**Supporting Information Available:** Labeling of PARP-1 with <sup>32</sup>P-NAD, labeling of PARP-1 truncations by PARP-1, the time course and the detection limit of the labeling reaction, confirmation of PARP-1 KD in MCF-7 cells, synthesis of Biotin-N<sub>3</sub>, the full list of identified potential PARP-1 substrate proteins. This material is available free of charge via the Internet at <http://pubs.acs.org>.

JA101588R